



Effect of B-ring substitution pattern on binding mode of propionamide selective androgen receptor modulators

Casey E. Bohl^a, Zengru Wu^a, Jiyun Chen^a, Michael L. Mohler^b, Jun Yang^a, Dong Jin Hwang^b, Suni Mustafa^b, Duane D. Miller^b, Charles E. Bell^c, James T. Dalton^{a,*}

^a Division of Pharmaceutics, College of Pharmacy, The Ohio State University, 500 West 12th Avenue, 242 L.M. Parks Hall, Columbus, OH 43210, USA

^b Department of Pharmaceutical Sciences, College of Pharmacy, University of Tennessee, Memphis, TN 38163, USA

^c Department of Molecular and Cellular Biochemistry, College of Medicine and Public Health, The Ohio State University, Columbus, OH 43210, USA

ARTICLE INFO

Article history:

Received 28 July 2008

Revised 28 August 2008

Accepted 2 September 2008

Available online 5 September 2008

Keywords:

Androgen receptor

Crystallography

Prostate cancer

Cachexia

SARM

ABSTRACT

Selective androgen receptor modulators (SARMs) are essentially prostate sparing androgens, which provide therapeutic potential in osteoporosis, male hormone replacement, and muscle wasting. Herein we report crystal structures of the androgen receptor (AR) ligand-binding domain (LBD) complexed to a series of potent synthetic nonsteroidal SARMs with a substituted pendant arene referred to as the B-ring. We found that hydrophilic B-ring *para*-substituted analogs exhibit an additional region of hydrogen bonding not seen with steroidal compounds and that multiple halogen substitutions affect the B-ring conformation and aromatic interactions with Trp741. This information elucidates interactions important for high AR binding affinity and provides new insight for structure-based drug design.

© 2008 Elsevier Ltd. All rights reserved.

Pharmacological agents that mimic the effects of endogenous androgens provide treatment options for numerous diseases involving AR regulation. Testosterone replacement therapy is given to patients with androgen deficiencies often as a patch or gel due to its poor oral bioavailability.^{1–3} Side effects from testosterone treatment including hair loss, gynecomastia, and prostate hyperplasia stem from metabolism to dihydrotestosterone (DHT) by 5 α -reductase or aromatization to estrogenic metabolites, limiting its use in other AR regulated disorders.^{4–6} Nonsteroidal propionamide antiandrogens such as bicalutamide are commonly used in treatment of prostate cancer and provide advantages over steroidal antagonists due to oral bioavailability and lack of cross-reactivity with other steroid receptors.⁶ Nonsteroidal AR agonists would provide similar benefits over traditional testosterone therapy as well as avoid conversion to DHT and estradiol. In vivo studies conducted in our laboratory demonstrate that a series of nonsteroidal androgens selectively increase muscle size relative to prostate and seminal vesicles offering clinical potential for treating acute muscle wasting and sarcopenia.^{1,7–10}

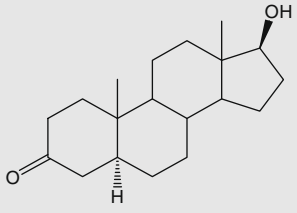
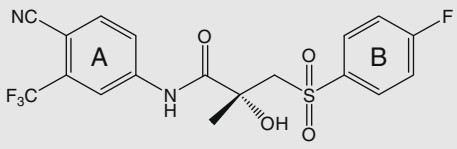
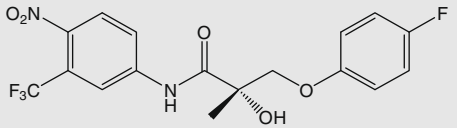
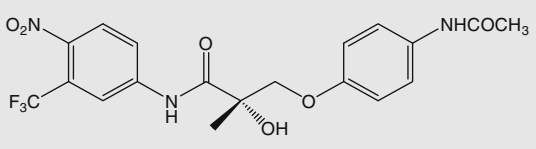
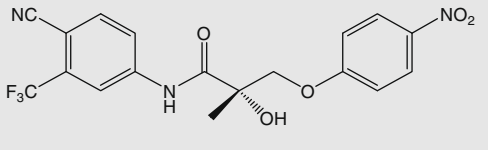
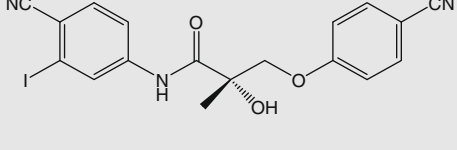
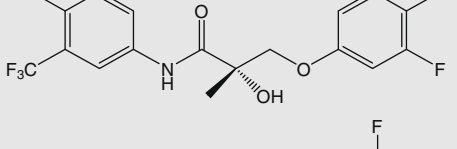
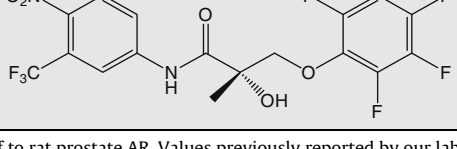
Design, synthesis, and evaluation of a large number of aryl propionamides led to refinement of structure–activity relationships for these SARMs.^{11–13} We discovered that modification of the sulfonyl group of bicalutamide to a thio- or ether-linkage group re-

sulted in agonist activity as witnessed by AR-mediated transcription.^{12–14} In vivo experiments showed that the ether-linked compounds offered more favorable responses due to metabolic and pharmacokinetic profiles.^{13,15,16} Results also indicated that ether-linked bicalutamide analogs elicit greater effects in anabolic tissue (e.g., muscle and bone) than androgenic tissue (e.g. prostate and seminal vesicles) as compared to DHT treated, castrated rats.^{7,15,16} Furthermore, we found that hydrophilic substituents on the *para*-position of the B-ring including an acetamido, a cyano, or a nitro group¹⁵ increase binding affinities and that further modification of the B-ring with electron-withdrawing groups^{8,17} was also favorable (Table 1). Recently, we reported crystal structures of nonsteroidal ligands complexed to the AR, which provided a basis for how the ether-linked bicalutamide agonist derivative, S-1 could be accommodated in the AR.¹⁸ To advance our understanding as to why B-ring substituted S-1 derivatives resulted in significantly higher AR binding affinities, we solved the X-ray crystal structures of the AR LBD complexed to ligands containing a *para*-substituted acetamido (S-4), nitro (S-21), and cyano group (S-24), as well *p*-chloro-*m*-fluoro (C-31) and penta-fluoro (C-23) B-ring substituted analogs. Herein we describe the AR interactions that distinguish these ligands in terms of high binding affinities, which progresses the understanding of the AR binding pocket and provides new information for rational drug design.

The *R*-3-bromo-*N*-(4-cyano (or 4-nitro)-3-trifluoromethylphenyl)-2-hydroxy-2-methylpropionamides were synthesized as

* Corresponding author. Tel.: +1 614 688 3797; fax: +1 614 292 7766.
E-mail address: dalton.1@osu.edu (J.T. Dalton).

Table 1
Chemical structures and binding affinities

		K_i (nM)
DHT		0.27
R-bicalutamide		11±2
S-1		6.1±0.2
S-4		4.0±0.7
S-21		2.5±0.2
S-24		0.54±0.03
C-31		1.7±0.2
C-23		1.4±0.3

Binding affinity determined by competitive inhibition of to rat prostate AR. Values previously reported by our laboratory include R-bicalutamide²³, S-1¹³, S-4⁷, S-21²⁴, and C-23.²²

previously reported by Kirkovsky et al.¹⁹ Target compounds S-1, S-4, S-21, C-23, and C-31 were synthesized by modifications of the methods previously published by Marhefka et al.¹³ and Nair et al.,²⁰ respectively (see [Supplementary Data](#) for details). Crystals of the AR LBD SARM complexes were obtained using previously published methods^{18,21} as described in the [Supplementary Data](#). Crystallography statistics are shown in [Table 2](#).

Previous reports of structure–activity relationships for nonsteroidal AR ligands demonstrate that hydrogen bond acceptor groups

on the *para* position of the A-ring are important for high binding affinity to the AR.^{11,12} The nitro and cyano groups on hydroxyflutamide and R-bicalutamide, respectively, were therefore preserved in our optimization of nonsteroidal AR ligands. X-ray crystal structures demonstrate hydrogen bonds between the A-ring cyano groups of S-21, S-24, and C-31 to Arg752 of helix 5, and to a water molecule ([Fig. 1](#)) resembling the interactions with the cyano group of R-bicalutamide binding to the W741L AR.²¹ The nitro group on S-4 and C-23 are however within hydrogen bond range to

Table 2
Crystallographic data and refinement statistics

Drug	S-4	S-21	S-24	C-31	C-23
PDB Code	3b68	3b66	3b65	3b5r	3b67
Spacegroup	P2 ₁ 2 ₁ 2 ₁				
Unit cell					
<i>a</i>	54.73	54.74	54.64	54.89	54.86
<i>b</i>	66.57	66.60	66.71	66.80	66.20
<i>c</i>	68.64	69.10	69.04	69.16	69.74
Resolution range (Å)	23.75–1.90 (1.97–1.90) ^a	23.98–1.65 (1.71–1.65) ^a	26.32–1.80 (1.86–1.80) ^a	22.01–1.80 (1.86–1.80) ^a	29.90–1.90 (1.97–1.90) ^a
Number of unique reflections	20,381	30,834	23,944	23,820	20,501
Average redundancy	7.03 (7.00)	5.98 (4.59)	13.85 (13.92)	9.12 (5.58)	6.93 (6.50)
% completeness	100.0 (100.0)	99.2 (95.1)	99.5 (98.6)	98.3 (86.8)	99.3 (97.2)
<i>R</i> _{merge} ^b	0.159 (0.443)	0.089 (0.424)	0.144 (0.382)	0.129 (0.328)	0.141 (0.441)
<i>I</i> / σ	6.6 (3.4)	10.9 (3.2)	12.1 (6.7)	10.4 (4.6)	9.2 (4.0)
<i>R</i> factor ^c	0.234 (0.390)	0.213 (0.333)	0.242 (0.425)	0.233 (0.393)	0.226 (0.375)
<i>R</i> _{free}	0.274 (0.400)	0.242 (0.351)	0.292 (0.424)	0.272 (0.409)	0.273 (0.393)
rmsd bonds (Å)	0.007	0.006	0.006	0.006	0.006
rmsd angles	1.1	1.1	1.1	1.1	1.1
mean <i>B</i> value (Å ²)	23.0	20.0	21.9	20.2	23.2

^a Values for data in the last resolution shell shown in parenthesis.

^b $R_{\text{merge}} = \sum |I_h - \langle I \rangle_h| / \sum I_h$, where $\langle I \rangle_h$ is average intensity over symmetry equivalents.

^c $R\text{-factor} = \sum |F_{\text{obs}} - F_{\text{calc}}| / \sum F_{\text{obs}}$. The free *R*-factor was calculated from 10% of the reflections that were omitted from the refinement.

Arg752 and the water molecule as well as Gln711 on helix 3 mimicking interactions seen with S-1.¹⁸ Hydrogen bonds involving the

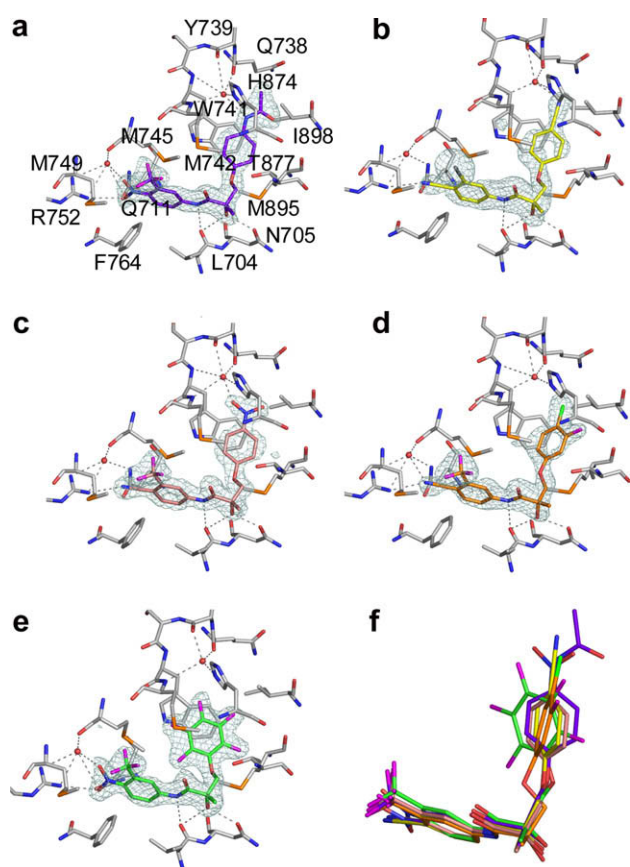


Figure 1. Comparison of SARM binding conformations to the AR. (a) S-4 (carbons—purple), (b) S-24 (carbons—yellow), (c) S-21 (carbons—salmon), (d) C-31 (carbons—orange), (e) C-23 (carbons—green) fit into $F_o - F_c$ simulated annealing omit maps. AR carbons—gray; nitrogens—blue; oxygens—red; sulfurs—orange; fluorines—magenta; chlorine—green. Possible hydrogen bonds within 3.5 Å depicted as dashed lines. Each of the compounds forms hydrogen bonds to Arg752, Leu704, and Asn705. SARMs with a nitro substituent on the A-ring (i.e., S-4, S-21, and C-23) also form a hydrogen bond to Gln711. SARMs with a hydrophilic B-ring substituent (i.e. S-4, C-21, and C31) form a hydrogen bond to a water molecule that is stabilized by His874 and backbone residues of helices 4 and 5. (f) Overlap of the bound conformations of these SARMs portrays the different B-ring orientations.

amide nitrogen and chiral hydroxyl group interacting with Leu704 and Asn705 are conserved in this series of nonsteroidal ligands resembling hydroxyflutamide and bicalutamide and provide the basis for the stereo-selective binding of these compounds. Presence of a hydrophobic substituent on the *meta*-position of the A-ring, which has been shown important for maintaining high binding affinity,^{11,12} was maintained with a trifluoromethyl group on compounds S-4, S-21, C-31, and C-23 and an iodine atom on S-24. The iodine at this position on S-24 mimics the trifluoromethyl substituted ligands as seen from similar binding affinities of these derivatives¹¹ and similar Van der Waals contacts in the X-ray crystal structures.

Screening of B-ring substituted propionamide SARMs demonstrated that halogens could be placed anywhere on the B-ring of SARMs, while hydrophilic electron withdrawing substituents were only found favorable on the *para* position.^{11,22} Crystal structures of S-4, S-21, and S-24 reveal that the hydrophilic B-ring substituent hydrogen bonds to a water molecule located in a kink between helices 4 and 5, which also hydrogen bonds to His874 (Fig. 1a–c). The improved binding affinities of these compounds over S-1 is therefore likely attributed to the stronger hydrogen bonding properties of the acetamido, cyano, and nitro substitutions compared to a fluorine. The nitro and cyano groups of compounds S-21 and S-24, respectively, act as hydrogen bond acceptors, while the acetamide on S-4 can act as both a hydrogen bond donor and acceptor. The lone pair of electrons on the acetamide nitrogen of S-4 thus presumably accepts a hydrogen from the water molecule mimicking the interactions seen with the nitro and cyano substituents, which would explain the poor binding affinity of amine substitutions on the *para* position of the B-ring.^{11,12} The significantly higher binding affinity of S-24 and S-21 relative to S-4 appears to be a result of the extra bulk on the acetamido group. Steric clash of the S-4 acetamide with Val903 causes a turn in the B-ring. In addition, the acetyl portion of the acetamide group on S-4 is oriented such that the oxygen atom displaces the Ile898 side chain relative to the other structures (Fig. 2a) to allow its accommodation within the binding pocket. This interaction pushes helix 12 away from the binding pocket approximately 2 Å relative to the other AR LBD-SARM complexes. Also, the methyl group of the acetamide is unfavorably situated only 3.1 Å from the backbone oxygen of Gln738. Further optimization of the *para* substituent therefore may be possible to exploit a hydrogen bond to the backbone oxygen of Gln738. The B-ring of S-21 and S-24 share nearly the same orientation. However, the nitro group on the *para* position of S-21

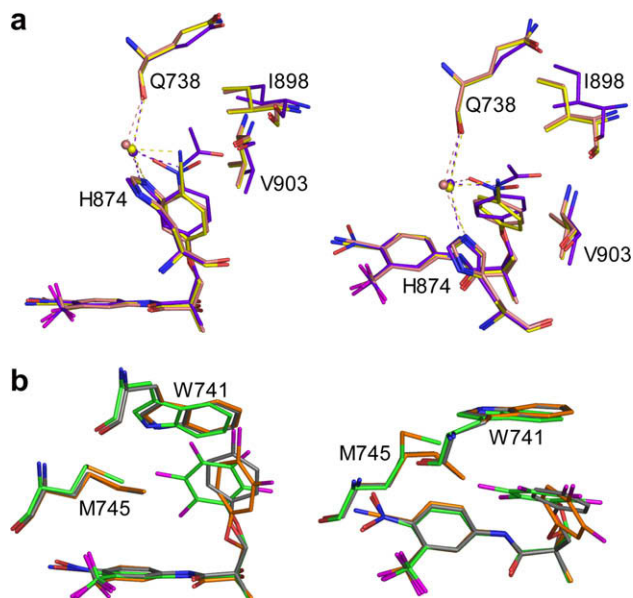


Figure 2. AR-SARM complexes seen in multiple orientations. (a) Overlay of S-4 (purple), S-21 (salmon), and S-24 (yellow) demonstrating interactions between the B-ring *para* substituent and residues His874, Ile898, Val903, and the backbone of Gln738. Notice that each of these ligands hydrogen bonds to a conserved water molecule in this region. The acetamido group on S-4 forms close contacts with the side chains of Ile898 and Val903 inducing a slight displacement of helix 12. (b) Overlay of S-1 (black, PDB code 2AXA¹⁸), C-31 (orange), and C-23 (green) demonstrating differences in B-ring orientations with respect to Trp741. Substitution of a fluorine on the *meta* position of the B-ring in C-31 causes the B-ring to turn relative to S-1. This orientation of the B-ring appears to result in an edge-to-face aromatic ring interaction with Trp741 possibly due to the increased acidity of the remaining hydrogen atom on the *meta* position. C-23 contains a completely fluorine substituted B-ring, which orients nearly parallel to the Trp741 indole ring creating a π - π interaction and results in displacement of the Met745 side chain. Additionally, the fluorine on the *ortho* position seems to be acting as a hydrogen bond acceptor pulling the B-ring of C-23 towards the amide nitrogen of the compound.

is observed less than 3.0 Å from the Val903 side chain in the X-ray crystal structure. This steric interaction is alleviated in the S-24 bound AR in which the cyano group is situated over 3.5 Å from the Val903 side-chain. However, structure-activity relationships have shown very little difference in binding affinity between a cyano and nitro at this position.¹⁵ Instead, the iodine on the *meta* position of the A ring appears to be the reason for the increased affinity of S-24 over S-21.

C-31 and C-23 exhibit significantly higher AR binding affinity than S-1 as a result of multiple halogen substitutions on the B-ring. The electron withdrawing effect and/or increased Van der Waals contacts with these analogs therefore cause increases in AR binding affinities. The B-ring was observed in a slightly different orientation in each of the halogen substituted compounds when bound to the AR (Figs. 1d, e, f and 2b). The C-31 B-ring is rotated compared with compound S-1 to accommodate the *meta* fluorine in a cavity between Thr877, Ile899, and Val903. Conversely, the B-ring of C-23 is not rotated relative to S-1, but instead is positioned towards Met745 resulting in its displacement (Fig. 2b). A plausible explanation is that the higher binding affinities of these multi-substituted halogen derivatives results in favorable interactions with the Trp741 side chain. Interestingly, the B-ring of C-31 turns relative to S-1 to become nearly perpendicular to the indole ring of Trp741. The additional electron-withdrawing effect of the *meta* halogen would increase the acidity of the aromatic hydrogen for formation of a edge-to-face aromatic ring interaction with Trp741. Conversely, the B-ring of C-23 is completely substituted abolishing the capability for this edge interaction. The C-23 B-ring

is observed almost parallel and aligned for π - π stacking. Moreover, the *ortho* fluorine on the side facing Met745 was observed 3.1 Å from the amide nitrogen suggesting that the B-ring may be pulled toward the amide by an intramolecular hydrogen bond (Figs. 1e and 2b).

The crystal structures presented herein demonstrate favorable interactions in a subpocket of the AR unoccupied by steroidal androgens. An additional region of hydrogen bonding not available to endogenous AR ligands provides the potential for increasing nonsteroidal ligand binding affinities beyond that of the most potent endogenous androgen, DHT. Higher binding affinities observed with SARMs containing multiple halogen substituted B-rings may be attributed to π - π stacking and edge-to-face interactions with Trp741, as well as increased Van der Waals contacts. Further optimization of propionamide SARMs will however conceivably require exploitation of increased hydrophobic interactions and hydrogen bonding to Thr877 similar to steroidal ligands in addition to interactions with Trp741, His874, and potentially even Gln738.

Acknowledgment

Supported by NIH Grants R01 DK59800 and R01 DK065227.

Supplementary data

Supplementary data associated with this article can be found, in the online version, at doi:10.1016/j.bmcl.2008.09.002.

References and notes

- Gao, W.; Reiser, P. J.; Coss, C. C.; Phelps, M. A.; Kearbey, J. D.; Miller, D. D.; Dalton, J. T. *Endocrinology* **2005**.
- Jockenovel, F. *Aging Male* **2003**, *6*, 200.
- Swerdloff, R. S.; Wang, C.; Cunningham, G.; Dobs, A.; Iranmanesh, A.; Matsumoto, A. M.; Snyder, P. J.; Weber, T.; Longstreth, J.; Berman, N. J. *Clin. Endocrinol. Metab.* **2000**, *85*, 4500.
- Tan, R. S.; Culberson, J. W. *Maturitas* **2003**, *45*, 15.
- Wang, C.; Swerdloff, R. S. *J. Clin. Endocrinol. Metab.* **2002**, *87*, 1462.
- Gooren, L. J.; Bunck, M. C. *Drugs* **2004**, *64*, 1861.
- Yin, D.; Gao, W.; Kearbey, J. D.; Xu, H.; Chung, K.; He, Y.; Marhefka, C. A.; Veverka, K. A.; Miller, D. D.; Dalton, J. T. *J. Pharmacol. Exp. Ther.* **2003**, *304*, 1334.
- Chen, J.; Hwang, D. J.; Bohl, C. E.; Miller, D. D.; Dalton, J. T. *J. Pharmacol. Exp. Ther.* **2004**.
- Kearbey, J. D.; Gao, W.; Narayanan, R.; Fisher, S. J.; Wu, D.; Miller, D. D.; Dalton, J. T. *Pharm. Res.* **2006**.
- Bhasin, S.; Calof, O. M.; Storer, T. W.; Lee, M. L.; Mazer, N. A.; Jasuja, R.; Montori, V. M.; Gao, W.; Dalton, J. T. *Nat. Clin. Pract. Endocrinol. Metab.* **2006**, *2*, 146.
- Bohl, C. E.; Chang, C.; Mohler, M. L.; Chen, J.; Miller, D. D.; Swaan, P. W.; Dalton, J. T. *J. Med. Chem.* **2004**, *47*, 3765.
- Yin, D.; He, Y.; Perera, M. A.; Hong, S. S.; Marhefka, C.; Stourman, N.; Kirkovsky, L.; Miller, D. D.; Dalton, J. T. *Mol. Pharmacol.* **2003**, *63*, 211.
- Marhefka, C. A.; Gao, W.; Chung, K.; Kim, J.; He, Y.; Yin, D.; Bohl, C.; Dalton, J. T.; Miller, D. D. *J. Med. Chem.* **2004**, *47*, 993.
- Dalton, J. T.; Mukherjee, A.; Zhu, Z.; Kirkovsky, L.; Miller, D. D. *Biochem. Biophys. Res. Commun.* **1998**, *244*, 1.
- Kim, J.; Wu, D.; Hwang, D. J.; Miller, D. D.; Dalton, J. T. *J. Pharmacol. Exp. Ther.* **2005**, *315*, 230.
- Gao, W.; Kearbey, J. D.; Nair, V. A.; Chung, K.; Parlow, A. F.; Miller, D. D.; Dalton, J. T. *Endocrinology* **2004**, *145*, 5420.
- Chen, J.; Hwang, D. J.; Chung, K.; Bohl, C. E.; Fisher, S. J.; Miller, D. D.; Dalton, J. T. *Endocrinology* **2005**.
- Bohl, C. E.; Miller, D. D.; Chen, J.; Bell, C. E.; Dalton, J. T. *J. Biol. Chem.* **2005**, *280*, 37747.
- Kirkovsky, L.; Mukherjee, A.; Yin, D.; Dalton, J. T.; Miller, D. D. *J. Med. Chem.* **2000**, *43*, 581.
- Nair, V. A.; Mustafa, S. M.; Mohler, M. L.; Fisher, S. J.; Dalton, J. T.; Miller, D. D. *Tetrahedron Lett.* **2004**, *45*, 9475.
- Bohl, C. E.; Gao, W.; Miller, D. D.; Bell, C. E.; Dalton, J. T. *Proc. Natl. Acad. Sci. U.S.A.* **2005**, *102*, 6201.
- Chen, J.; Hwang, D. J.; Chung, K.; Bohl, C. E.; Fisher, S. J.; Miller, D. D.; Dalton, J. T. *Endocrinology* **2005**, *146*, 5444.
- Mukherjee, A.; Kirkovsky, L.; Yao, X. T.; Yates, R. C.; Miller, D. D.; Dalton, J. T. *Xenobiotica* **1996**, *26*, 117.
- Kim, J.; Wu, D.; Hwang, D. J.; Miller, D. D.; Dalton, J. T. *J. Pharmacol. Exp. Ther.* **2005**.